THE JOURNAL OF BIOLOGICAL CHEMISTRY

Vol. 279, No. 32, Issue of August 6, pp. 33630–33638, 2004
Printed in U.S.A.

Probing the Specificity of the Subclass B3 FEZ-1 Metallo-β-lactamase by Site-directed Mutagenesis*

Received for publication, April 2, 2004, and in revised form, May 19, 2004
Published, JBC Papers in Press, May 24, 2004, DOI 10.1074/jbc.M403671200

Paola Sandra Mercuri‡, Isabel García-Sáez§, Kris De Vriendt¶, Iris Thamm‡, Bart Devreese¶, Jozef Van Beeumen¶, Otto Dideberg§, Gian Maria Rossolini‖, Jean-Marie Frère‡, and Moreno Galleni‡**

From the ‡Centre d'Ingénierie des Protéines, B6 Sart Tilman, Université de Liège, B-4000 Liège, Belgium, §Institut de Biologie Structurale Jean-Pierre Ebel (CNRS-CEA-UJF), 38027 Grenoble Cedex-France, ¶Laboratory of Protein Biochemistry and Protein Engineering, University of Gent, K. L. Ledeganckstraat 35, B-9000 Gent, Belgium, and ‖Dipartimento di Biologia Molecolare, Sezione di Microbiologia, Università di Siena, I-53100 Siena, Italy

The subclass B3 FEZ-1 β-lactamase produced by *Fluoribacter* (*Legionella*) *gormanii* is a Zn(II)-containing enzyme that hydrolyzes the β-lactam bond in penicillins, cephalosporins, and carbapenems. FEZ-1 has been extensively studied using kinetic, computational modeling and x-ray crystallography. In an effort to probe residues potentially involved in substrate binding and zinc binding, five site-directed mutants of FEZ-1 (H121A, Y156A, S221A, N225A, and Y228A) were prepared and characterized using metal analyses and steady state kinetics. The activity of H121A is dependent on zinc ion concentration. The H121A monozinc form is less active than the dizinc form, which exhibits an activity similar to that of the wild type enzyme. Tyr^{156} is not essential for binding and hydrolysis of the substrate. Substitution of residues Ser^{221} and Asn^{225} modifies the substrate profile by selectively decreasing the activity against carbapenems. The Y228A mutant is inhibited by the product formed upon hydrolysis of cephalosporins. A covalent bond between the side chain of Cys^{200} and the hydrolyzed cephalosporins leads to the formation of an inactive and stable complex.

Metallo-β-lactamases are bacterial enzymes that hydrolyze antibiotics of the β-lactam family. They are classified as class B (1) or group 3 (2) β-lactamases. In the last decade, the discovery of an increasing number of new metallo-β-lactamases resulted in a subdivision into three molecular subclasses: B1, B2, and B3. Thereafter, a standard numbering scheme (3) was adopted that identifies conserved residues involved in the catalytic activity. Subclass B3 β-lactamases are broad spectrum enzymes that require one or two Zn (II) ions for activity (4). These enzymes are produced by various environmental species, of which some can cause opportunistic infections (such as *S. maltophilia* (5) and *F. gormanii* (6)), whereas others are not pathogenic such as *Janthinobacterium lividum* (7) and *Caulobacter crescentus* (8, 9). The structures of several subclass B1 β-lactamases have been solved by x-ray crystallography (BcII (10, 11), CcrA (12), BlaB (13), and IMP-1 (14)). To date, no structure of a subclass B2 enzyme is available. In subclass B3, the crystal structures of the metallo β-lactamases L1 from *S. maltophilia* (15) and FEZ-1 from *F. gormanii* (16) have been solved. Comparison of the tertiary structures of the different enzymes highlighted similar organizations of the secondary structure elements; they all contain an αββα sandwich with two central β-sheets and α-helices on the external faces (10). The active site with the binuclear zinc center is located at the bottom of the β-sheet core. Zn1 is tetrahedrally coordinated by three histidines, His^{116}, His^{118}, His^{196}, and a water molecule. In the subclass B1 enzymes, Zn2 is coordinated by His^{263}, Asp^{120}, Cys^{221}, and two water molecules to form a trigonal bipyramid. In subclass B3 β-lactamases, a Ser residue replaces Cys^{221}, and His^{121} is the third ligand of Zn2. Our studies were performed on the FEZ-1 β-lactamase. FEZ-1 is a monomeric enzyme. The sequence of the mature protein is easily aligned with that of the L1 enzyme with 33% of isology (17). The two subclass B3 β-lactamases exhibit a broad activity spectrum against β-lactam antibiotics, but FEZ-1 shows a preference for cephalosporins (18), whereas the L1 β-lactamase seems to be more active against penicillins (19, 20). Comparison of the x-ray structures reveals similar zinc binding sites in FEZ-1 and L1. In L1, Ullah et *al*. (15) postulate that the carbonyl oxygen of the β-lactam substrate interacts with an oxyanion hole formed by Zn-1 and the side chain of Tyr^{228}. This tyrosine is conserved and could play the same role in FEZ-1. In L1, the β-substituent on C-6 or C-7 of the β-lactam substrate generally fits in a hydrophobic pocket formed by the "flap" connecting β_3 and β_4, and by the loop between β_3 and β_8, which is considerably longer in subclass B3 enzymes than in subclass B1 (21, 22). In this pocket, the hydrophobic residues Phe^{156} and Ile^{162} of L1 are replaced by a Tyr and a Ser residue, respectively, in FEZ-1. These substitutions, together with Asn^{225}, should influence the substrate specificity, with a facilitated interaction between FEZ-1 and β-lactams bearing a less hydrophobic β side chain (15). With the exception of GOB-1, all of the subclass B3 enzymes have a serine at position 221 (23). The x-ray structures of L1 (15) and FEZ-1 (16) indicate that this residue interacts with a water molecule (Wat2) linked to Zn2. Modeling studies suggest that Wat2 might play the role of proton donor to the nitrogen of the β-lactam ring. The interaction with Ser^{221} should help its positioning in the catalytic cavity. A typical structural aspect of L1 when compared with the other class B β-lactamases is the presence of an intramolecular disul-

* This work was supported in part by European Union Grant HPRN-CT-2002 00264 as part of the Research Training Networks Program; by Belgian Program Pôles d'Attraction Interuniversitaire (initiated by the Belgian State, Prime Minister's Office) Grant PAI P5/33; and by Fund for Scientific Research Flanders Grant G. 0312.02. The costs of publication of this article were defrayed in part by the payment of page charges. This article must therefore be hereby marked "*advertisement*" in accordance with 18 U.S.C. Section 1734 solely to indicate this fact.

The nucleotide sequence(s) reported in this paper has been submitted to the GenBank™/EBI Data Bank with accession number(s) 1K07 and 1L9Y.

** To whom correspondence should be addressed: Centre d' Ingénierie des Proteines, B6 Sart Tilman, Université de Liège, B-4000 Liège, Belgium. Tel.: 32-4-3663419; Fax: 32-4-3663364; E-mail: mgalleni@ulg.ac.be.

TABLE I

Mutagenic primers (5′ → 3′) used for the constructions of the FEZ-1 mutants. The modified bases are in boldface type and underlined

Primers	Nucleotidic sequences
H121A$_{for}$	CCTATGCTCATTTTGATGCTGCGGCCGGTAGCG
H121A$_{rev}$	CGCTACCGGCCGCAGCATCAAAATGAGCATAGG
S221A$_{for}$	ATCAGGCCGTAATTATAGGA**GC**TATTGGCGTAAATCCTTGGG
S221A$_{rev}$	CCCAAGGATTTACGCCAATA**GC**TCCTATAATTACGGCCTGAT
C200A$_{for}$	CCTGGACACACTAGAGGC**GC**TACCACCTGGACAATGAAAC
C200A$_{rev}$	GTTTCATTGTCCAGGTGGTA**GC**GCCTCTAGTGTGTCCAGG
Y156A$_{for}$	CTGTCTGGCGGTAAATCTGATTTTCAT**GC**TGCTAATGATTCC
Y156A$_{rev}$	GGAATCATTAGCA**GC**ATGAAAATCAGATTTACCGCCAGACAG
S162A$_{for}$	CATTATGCTAATGATTCC**GC**TACTTATTTTACTCAGAGTACTGTGGAT
S162A$_{rev}$	ATCCACAGTACTCTGAGTAAAATAAGTA**GC**GGAATCATTAGCATAATG
N225A$_{for}$	GGAAGTATTGGCGTA**GC**TCCTGGGTATAAATTGGTT
N225A$_{rev}$	AACCAATTTATACCCAGGA**GC**TACGCCAATACTTCC
Y228A$_{for}$	GGAGGTATTGGCGTAAATCCTGGG**GC**TAAATTGGTTGATAAT
Y228A$_{rev}$	ATTATCAACCAATTTA**GC**CCCAGGATTTACGCCAATACCTCC

fide bridge between Cys^{256} and Cys^{296}. These residues are conserved in FEZ-1, but this enzyme contains an additional Cys^{200} close to the active site. Finally, L1 and FEZ-1 are a homotetramer and a monomer, respectively. In the L1 structure, one main interaction between two subunits involves the N terminus (15, 24). However, this structural motif is missing in FEZ-1. In this paper, we have studied the role of residues His^{121}, Tyr^{156}, Ser^{221}, Asn^{225}, and Tyr^{228} in the catalytic activity of FEZ-1.

MATERIALS AND METHODS

Bacterial Strains and Vectors—The *Escherichia coli* XL-1 Blue (Stratagene Inc., La Jolla, CA) and *E. coli* BL21(DE3) pLysS (Novagen Inc., Madison, WI) strains were used as hosts for the construction of vectors for the expression of all of the studied proteins. The pDML1810 plasmid described previously by Mercuri *et al.* (18) was used as template in the PCR site-directed mutagenesis amplifications. The expression vector pET26b(+) (Novagen) was used for the construction of the T7-based expression plasmid.

Chemicals and Antibiotics—The primers used for the mutagenesis were synthesized by Amersham Biosciences. The QuikChange™ site-directed mutagenesis kit was from Stratagene (La Jolla, CA), and the isopropyl-β-thiogalactopyranoside was purchased from Eurogentech (Liège, Belgium). Chloramphenicol, ampicillin ($\Delta\epsilon_{235}$ = −820 M^{-1} cm^{-1}), cephalothin ($\Delta\epsilon_{260}$ = −6500 M^{-1} cm^{-1}), cefotaxime ($\Delta\epsilon_{260}$ = −7500 M^{-1} cm^{-1}), and cefuroxime ($\Delta\epsilon_{235}$ = −7600 M^{-1} cm^{-1}) were purchased from Sigma, and benzylpenicillin ($\Delta\epsilon_{235}$ = −775 M^{-1} cm^{-1}) was a gift from Rhône-Poulenc (Paris, France). Kanamycin was purchased from Merck, imipenem ($\Delta\epsilon_{300}$ = −9000 M^{-1} cm^{-1}) was a gift from Merck Sharp and Dohme, meropenem ($\Delta\epsilon_{298}$ = −6500 M^{-1} cm^{-1}) was from ICI Pharmaceuticals (Macclefield, UK), and biapenem ($\Delta\epsilon_{294}$ = −9900 M^{-1} cm^{-1}) was from Wyeth Lederle (Tokyo, Japan). Nitrocefin ($\Delta\epsilon_{482}$ = +15,000 M^{-1} cm^{-1}) was purchased from Unipath Oxoid (Basingstoke, UK). 7-Aminocephalosporanic acid (7-ACA) ($\Delta\epsilon_{260}$ = −7500 M^{-1} cm^{-1}) was a gift from GlaxoSmithKline.

Site-directed Mutagenesis—The FEZ-1 mutants were obtained according to the instruction manual of the QuikChange™ site-directed mutagenesis kit from Stratagene (La Jolla, CA). The oligonucleotides (forward and reverse) used for the generation of the mutants are shown in Table I. PCR conditions were as follows: incubation at 95 °C for 30 s and 20 cycles of amplification (denaturation at 95 °C for 30 s, annealing at 55 °C for 1 min, and extension at 68 °C for 10 min). After amplification, the PCR fragments were digested by the DpnI restriction enzyme in order to eliminate all nonmutated DNA. The digested plasmids were used to transform *E. coli* XL-1 Blue competent cells, and colonies were isolated on Luria Bertani (25) agar plates containing 50 μg/ml each ampicillin and kanamycin. The nucleotide sequences of the desired mutants were verified by DNA sequencing. Thereafter, the plasmids were digested by the NcoI and BamHI restriction enzymes, and the fragments were ligated into the pET26b(+) vector previously digested by the same enzymes to yield pDML1817-H121A, pDML1819-C200A, pDML1820-S221A, pDML1825-Y156A, pDML1826-S162A, pDML1827-N225A, and pDML1828-Y228A. Finally, *E. coli* BL21 (DE3) pLysS cells were transformed with the plasmids containing the different mutations.

The mutant proteins were produced and purified as described for the wild type enzyme (18) in two purification steps. After the second step, the fractions that exhibited β-lactamase activity were collected and concentrated on a YM-10 membrane (Amicon, Beverly, MA) to a final concentration of about 1 mg/ml. Protein concentrations were determined using the BCA assay (Pierce), and the absorbance at 280 nm was also measured. The purity and the molecular masses of all purified proteins were confirmed by determining the molecular mass values with the help of an electrospray mass spectrometer (VG Bio-Q) upgraded with a Platform source (Micromass, Altrincham, UK). The samples (100 pmol) were dissolved in 0.05% formic acid, 50% acetonitrile in water and injected into the source of the mass spectrometer with a syringe pump (Harvard Instruments, South Natick, MA) at a flow rate of 6 μl/min.

Metal Content Analysis—The zinc content of the enzyme was measured by atomic absorption in the flame mode using a PerkinElmer 2100 spectrometer. Before the metal analyses, 1 ml of a 40 μM protein solution was dialyzed three times during 8 h at 4 °C against 1 liter of double-distilled metal-free water containing 10 mM cacodylate buffer, pH 6. The zinc content of this dialysis buffer was about 400 nM. The final dialysis buffers were used as blanks. Protein concentration was determined spectrophotometrically by using $\epsilon_{280\ nm}$ = 28,000 M^{-1} cm^{-1}. The metal content values reported for each sample are averages of results from three independent experiments.

Kinetic Studies—The hydrolysis of all antibiotics was monitored by following the absorbance variation resulting from the opening of the β-lactam ring, using a Uvikon 860 spectrophotometer equipped with thermostatically controlled cells and connected to a Copam PC 88C microcomputer. Cells with 0.2–1.0-cm path lengths were used depending on the substrate concentration. The kinetic parameters were determined either under initial rate conditions, using both Hanes' linearization of the Henri-Michaelis equation and a direct nonlinear regression with the hyperbolic equation or by analyzing the complete hydrolysis time courses, as described by De Meester *et al.* (26). The reported kinetic parameters values are the means of at least three experiments in which the different enzymes were added to the substrate solutions prepared in buffers containing the stated Zn^{2+} concentrations. All experiments were performed at 30 °C in 10 mM cacodylate, pH 6.0. Bovine serum albumin (20 μg/ml) was added to diluted β-lactamase solutions in order to prevent enzyme denaturation.

The heat stability of the different proteins was characterized. The enzymes (0.1 mg) were incubated at 50 °C in 10 mM cacodylate, pH 6.0. Aliquots were withdrawn after increasing periods of time, and the residual activity was measured against 1 mM benzylpenicillin.

Molecular Modeling—The S221A mutant model was based on the three-dimensional structure of FEZ-1 enzyme (16). The molecular model was built using the Homology module of the Insight program (Molecular Simulations, San Diego, CA), running on a Silicon Graphics work station. After model building, energy minimization was achieved using the Discover module of the same package to avoid bad molecular contacts. Finally, the geometric features were analyzed with the Insight II program.

Inhibition of Y228A Mutant by the Hydrolysis Cephalosporin Products—The progressive inactivation of the enzyme was monitored by analyzing the hydrolysis time course of different nitrocefin or cefuroxime concentrations in 10 mM sodium cacodylate, pH 6.0. In addition, 10 ml of 100 μM cefuroxime, cefotaxime, or cephalothin were hydrolyzed by 15 μg of FEZ-1 β-lactamase in 1 mM cacodylate buffer, pH 6. The hydrolysis of the cephalosporins was followed by recording the absorbance variation at 260 nm. After completion, the hydrolyzed antibiotics were separated from the enzyme by ultrafiltration on a YM-10 membrane (Amicon, Beverly, MA). The filtrates were collected and freeze-dried. The powders were resuspended in water to a final concentration of hydrolyzed product of 1 mM. The activity of the Y228A mutant was measured in the presence of different concentrations of the hydrolyzed cephalosporins. The variations of the pseudo-first-order inactivation

TABLE II

Kinetic parameters of the wild type enzyme (WT) and the H121A, Y156A, S221A, N225A, and Y228A FEZ-1 mutant enzymes

The measurements were performed in 15 mM cacodylate buffer, pH 6.0, at 30 °C. S.D. values were between 10 and 20%. ND, not determined.

Enzymes	Antibiotics	$[Zn^{2+}] \leq 0.4$ μM			$[Zn^{2+}] = 100$ μM		
		k_{cat}	K_m	k_{cat}/K_m	k_{cat}	K_m	k_{cat}/K_m
		s^{-1}	μM	$\mu M^{-1}\, s^{-1}$	s^{-1}	μM	$\mu M^{-1}\, s^{-1}$
WT	Benzylpenicillin	70	590	0.11	50	280	0.18
	Cefuroxime	320	50	6.6	330	35	9.4
	Cefotaxime	170	70	2.4	430	70	6.1
	Cephalothin	300	120	2.5	ND	ND	ND
	Nitrocefin	100	90	0.9	600	190	3.2
	7-ACA	30	1000	0.030	ND	ND	ND
	Imipenem	>200	>1000	0.2	>2000	>1000	2
	Meropenem	45	85	0.5	ND	ND	ND
	Biapenem	>70	>1000	0.07	ND	ND	ND
H121A	Benzylpenicillin	15	500	0.03	600	2200	0.27
	Cefuroxime	27	55	0.5	110	55	2.1
	Cefotaxime	60	100	0.6	120	60	2
	Nitrocefin	7	100	0.07	220	130	1.7
	Imipenem	>7	>1000	0.007	>70	>1000	0.07
Y156A	Benzylpenicillin	25	950	0.026	125	930	0.13
	Cefuroxime	550	60	9.2	820	125	6.5
	Cefotaxime	660	150	4.4	750	150	5
	Nitrocefin	190	130	1.5	50	20	2.4
	Imipenem	ND	ND	0.02	ND	ND	0.013
S221A	Benzylpenicillin	12	960	0.013	10	700	0.013
	Cefuroxime	160	85	1.9	480	360	1.3
	Cefotaxime	90	85	1.1	480	440	1.1
	Nitrocefin	8	80	0.1	85	240	0.35
	Imipenem	>2	>1000	0.002	>2	>1000	0.002
	Meropenem	0.3	115	0.003	ND	ND	ND
	Biapenem	>5	>1000	0.005	ND	ND	ND
N225A	Benzylpenicillin	25	600	0.04	20	800	0.03
	Cefuroxime	350	50	8	600	30	19
	Cefotaxime	800	120	7	1800	120	15
	Nitrocefin	16	20	0.8	60	180	3
	Imipenem	11	1250	0.01	5,5	800	0.007
	Meropenem	35	800	0.04	ND	ND	ND
	Biapenem	>4	>1000	0.004	ND	ND	ND
Y228A	Benzylpenicillin	125	3600	0.035	40	1300	0.03
	Cefuroxime	5900	160	35	6600	130	50
	Cefotaxime	1250	100	12,8	7600	660	11
	Cephalothin	2350	70	32	ND	ND	ND
	Nitrocefin	200	140	1.4	3250	65	50
	7-ACA	20	880	0.0024	ND	ND	ND
	Imipenem	>20	>1000	0.02	14	1000	0.014

rate constant k_i were also determined as a function of the hydrolyzed cephalosporin concentration (26).

Crystallization, Data Collection, and Structural Determination of the FEZ-1 Y228A Mutant—Crystals of the Y228A mutant were obtained by vapor diffusion in hanging drops at 8 °C by mixing 1 μl of protein (11 mg/ml) in 15 mM sodium cacodylate/cacodylic acid, pH 6.0, with 1 μl of 20% polyethylene glycol MME 5000, 0.2 M ammonium sulfate, 0.1 M sodium cacodylate/cacodylic acid, pH 6.0, and then adding 0.1 mM zinc acetate to a final concentration of 10 μM. Crystals were grown as needles, which reached dimensions of 500 × 30 × 30 μm in 3 weeks. They were monoclinic and belonged to space group $P2_1$, with unit cell parameters of a = 44.76 Å, b = 77.43 Å, c = 78.50 Å, $\alpha = \gamma = 90°$, β = 101.70°, with two molecules per asymmetric unit. A data set at 2.0 Å was collected using a Nonius FR-591 rotating anode x-ray generator running at 40 kV and 100 mA (λ = 1.5418Å), coupled to an image plate. The crystal was flash-frozen directly in the cryostream (100 K using an Oxford Cryosystems liquid nitrogen cryostat) after a short soaking in crystallization solution added with 20% glycerol. Data were processed and scaled using DENZO/SCALEPACK (27) and SCALA (28). The structure was solved by molecular replacement using CNS (29) tasks and a model of the wild-type FEZ-1 structure (16), with Tyr^{228} being replaced by Ala (16, 29). Cycles of model building, energy minimization, water-picking, and individual B-factor refinement using CNS gave a final model with $R_{working}$ = 18.6% and R_{free} = 21.6%, with ~10% of the data set aside for cross-validation.

MALDI-TOF[1] Measurements of Y228A Mutant and FEZ-1 WT—The mutant enzyme FEZ-1 Y228A and FEZ-1 WT (30 μM) were incubated with cefuroxime in a 1:1 ratio. The reaction was stopped after 15 min by denaturing the enzyme in 50% acetonitrile, 0.1% formic acid. The enzyme-cefuroxime complex was measured using a ESI-Q-TOF mass spectrometer (Micromass, UK), equipped with a nanospray source using gold/palladium-coated borosilicate needles purchased from Protana (Odense, Denmark). The capillary voltage was set at 1250 V, and the cone voltage was set at 40 V. Acquisition time was 2–3 min across an m/z range of 400–2500. The mass spectra were processed using the MassLynx version 3.1 software of Micromass.

For peptide mapping, the enzyme-cefuroxime complex (200 pmol) was diluted in 100 μl of 25 mM NH_4HCO_3, pH 8, and proteolyzed for 3 h at 37 °C by 0.1 μg of trypsin. For ESI-MS of the peptide mixture, the solution was diluted in 50% acetonitrile, 0.1% formic acid and measured using the ESI-Q-TOF MS as described above. For MALDI-TOF analysis, 1 μl of peptide solution was mixed with 1 μl of 50 mM α-cyano-4-hydroxycinnamic acid in 50% acetonitrile, 0.1% trifluoroacetic acid. A volume of 1 μl of this mixture was spotted on a metal target, dried in the air, and measured on a MALDI-TOF/TOF mass spectrometer (4700 Proteomics Analyzer; Applied Biosystems).

RESULTS AND DISCUSSION

Overexpression and Purification of FEZ-1 Mutants

The expression of all proteins was done in *E. coli* BL21(DE3) pLysS. Production of β-lactamases was tested at three temperatures, 37, 28, and 18 °C, in presence of 0.5 or 1 mM isopropyl-β-thiogalactopyranoside. Enzyme production was estimated by measuring the activity of crude extracts against cefuroxime and by SDS-PAGE. For the S162A and C200A variants, no

[1] The abbreviations used are: MALDI, matrix-assisted laser desorption ionization; TOF, time-of-flight; ESI, electrospray ionization; MS, mass spectrometry; 7-ACA, 7-aminocephalosporanic acid.

β-lactamase production was found either in soluble or insoluble form. These substitutions appeared to impede the correct folding of the protein and yielded an unstable protein. In the case of Ser[162], the comparison of the L1 and FEZ-1 structures reveals the presence of a two-residue insertion (Asn[159]-Asp[160]) in the FEZ-1 sequence (16). The insertion generates a very short 3_{10} helix stabilized by a hydrogen bond formed by the side chain interaction between Asp[160] and Ser[162]. In addition, Cys[200] is close to the active site and involved in a large network of hydrogen bonds.

For all of the other mutants, the maximal production in *E. coli* BL21(DE3) pLysS was obtained at 28 °C 6 h after the addition of 0.5 mM isopropyl-β-thiogalactopyranoside. The mutants were purified as described for the wild type FEZ-1 (17). The yields after purification could be estimated to be 4–8 mg/liter for the different enzymes.

Thermal Stability of Wild Type and Mutants of FEZ-1

At 30 °C the apparent stabilities of the WT and mutant enzymes were similar. At 50 °C, the Y156A, S221A, N225A, and Y228A mutants were rapidly inactivated ($t_{1/2} < 15$ min). In the case of mutant H121A, the enzyme was inactive after 15 min of incubation at 50 °C, but the addition of 100 μM zinc (final concentration) yielded an enzyme as stable as the wild type.

Zinc Content of the Different Mutants

Metal analyses of wild type FEZ-1 demonstrated that the enzyme binds 1.8 ± 0.2 Zn(II) ions per molecule. The Y156A, S221A, N225A, and Y228A mutants were found to also bind two zinc ions at an external zinc concentration of 0.4 μM. Under the same conditions, one zinc ion was found per H121A molecule. Thus, the substitution markedly reduced the affinity of the β-lactamase for the second zinc ion. Unexpectedly, despite the fact that all of the proteins but H121A appeared to contain a full complement of two zinc ions at an external zinc concentration of 0.4 μM, the addition of 100 μM Zn to the incubation medium significantly modified the kinetic parameters in a few cases. This observation remains presently unexplained unless one assumes that the opportunities for the second zinc might be specifically decreased by the substrate.

Substitution of a Zinc Ligand: The H121A Mutant

With the exception of benzylpenicillin, all of the K_m values were not dependent on the zinc ion concentration and were similar to those computed for the wild type enzyme (Table II). By contrast, at low [Zn^{2+}], the catalytic constant k_{cat} and the catalytic efficiencies k_{cat}/K_m of H121A were reduced 3–30-fold compared with the WT. The substitution of His[121] allowed the production of a monozinc form at low external concentration of metal ions. The addition of zinc to the reaction mixture increased the catalytic efficiency of H121A mainly by increasing the k_{cat} value. This behavior reflects the appearance of a dizinc H121A at high [Zn^{2+}], which was nearly as active as the wild type FEZ-1. The [Zn^{2+}] dependence of k_{cat} and K_m was measured with nitrocefin. As expected, K_m values remained constant for all of the tested [Zn^{2+}], but the k_{cat} values increased up to 5 μM. Further changes were observed at high [Zn^{2+}] (k_{cat} = 220 s^{-1} at [Zn] > 5 μM) (Fig. 1). Based on these data, we can postulate that the apparent dissociation constants for zinc of the monozinc and dizinc forms of H121A FEZ-1 are lower than 0.4 and 2.5 μM, respectively. The modification of a ligand for the second zinc ion thus had a strong impact on the catalytic properties of the enzyme. A similar although more important phenomenon was observed in the case of the *B. cereus* metallo-β-lactamase (BcII). In that enzyme, the replacement of Cys[221]

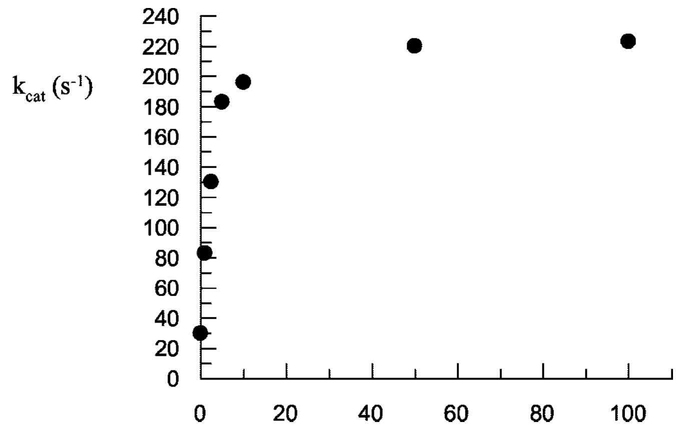

FIG. 1. **Dependence of the k_{cat} values of H121A on zinc ion concentrations.** The measurements were performed using 200 μM nitrocefin in 10 mM cacodylate buffer pH 6.0 at 30 °C. S.D. values were between 10 and 20%.

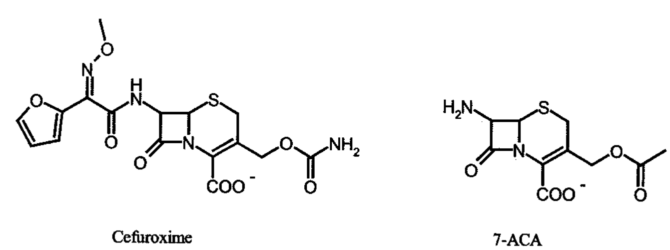

SCHEME 1

by alanine or serine yields a poorly active monozinc enzyme, whereas the dizinc form is nearly as active as the wild type BcII (30, 31). PAC and NMR experiments indicated that the cadmium ion can be found independently in both sites when less than one metal ion equivalent is added to the BcII apoenzyme (36). In addition, EXAFS experiments indicated that the same phenomenon is observed for the monzinc BcII (30). On the basis of all of the available data on FEZ-1 and other metallo-β-lactamases together, we propose that, in the monozinc form, the metal ion is alternatively located in both sites. The substitution of the histidine side chain modifies the affinity for zinc of the catalytic site. It could be possible that, in the presence of substrate, the zinc ion occupies the so-called second binding site at some stage during catalysis. Therefore, its integrity is needed to yield a fully active monozinc enzyme. The elimination of His[121] decreases the affinity of the second binding site and may favor an enzyme species where the zinc is mainly located in the first binding site. This phenomenon yields an enzyme with reduced catalytic efficiencies compared with the wild type FEZ-1. The addition of zinc ion allows the formation of a dizinc species and the restoration of a very active enzyme.

Substitution of Residues Involved in FEZ-1 Substrate Specificity

Effects of the Y156A Substitution—Only one major difference was observed between the Y156A mutant and the wild type FEZ-1 (Table II). A 10–100-fold decrease of k_{cat}/K_m for imipenem was noted depending on the zinc concentration. In contrast to that of the WT, the catalytic efficiency of the Y156A mutant toward imipenem was not significantly modified by increasing the metal ion concentration up to 100 μM. Crystallographic structures of metallo-β-lactamases highlight a flexible amino acid chain that extends over the active site. Studies of the CcrA (21, 22) and IMP-1 (14) enzymes show that this loop “clamps down” on inhibitors upon binding. A similar behavior is thus expected in the presence of the substrate. This phenom-

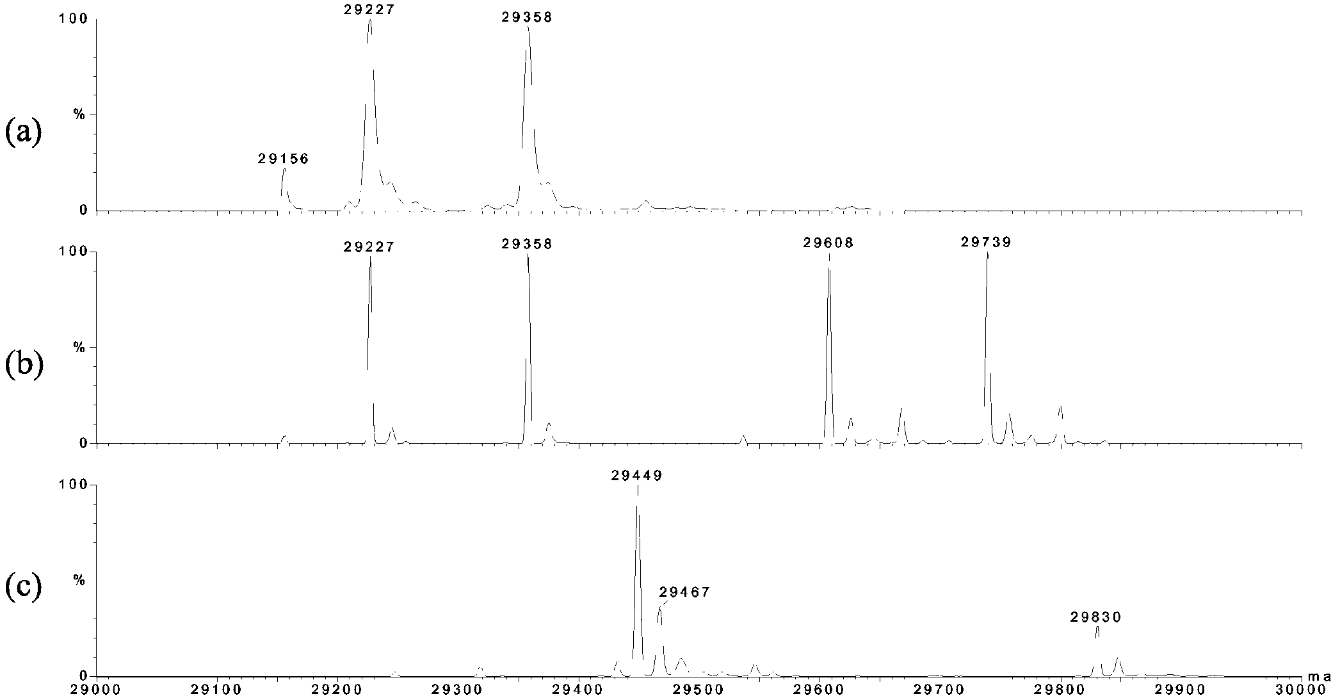

FIG. 2. **Deconvoluted ESI-MS spectrum of FEZ-1 Y228A (*a*), FEZ-1 Y228A incubated with cefuroxime (*b*), and FEZ-1 WT incubated with cefuroxime (*c*).** Note the mass shift of 381 Da after incubation with cefuroxime.

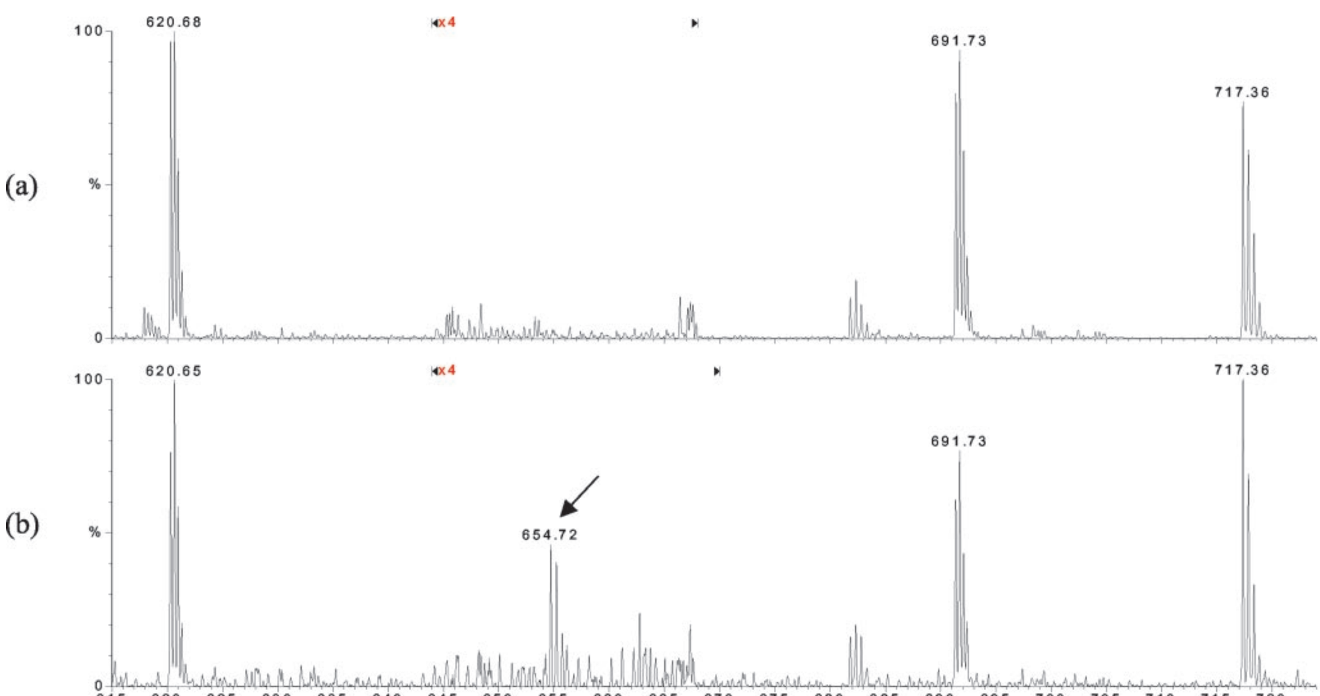

FIG. 3. **ESI-MS spectrum of the tryptic peptides of FEZ-1 Y228A (*a*) and FEZ-1 Y228A incubated with cefuroxime (*b*).** The *arrow* indicates a new doubly charged peptide, corresponding to a mass of 1307.4 Da.

enon may participate in determining the catalytic efficiency of the β-lactamases. The crystal structure of the L1 β-lactamase shows that there is a large loop that extends over the active site, and modeling studies have predicted that Phe[156] (for L1) and Tyr[156] (for FEZ-1) can make significant contacts with large substituents at the C-6 or C-7 positions in penicillins or cephalosporins, respectively. In L1, the F156A mutation yields a β-lactamase with a catalytic efficiency similar to that of the wild type (32). In consequence, the experimental data do not support the conclusions of the modeling studies (18).

Kinetic Properties of the S221A Mutant—The substitution of Ser[221] in alanine resulted in a modification of the FEZ-1 activity spectrum (Table II). Although somewhat decreased, the activities against cephalosporins and penicillins were well conserved. The K_m values for these antibiotics remained similar to those calculated for the wild type enzyme. The k_{cat} values were generally 2–10-fold lower than for the wild type enzyme. In contrast, the activity of S221A was poor against all tested carbapenems (imipenem, biapenem, and meropenem). The k_{cat}/K_m values were 10–100-fold lower than those of the wild type enzyme. The decrease of the catalytic efficiency *versus* meropenem was due to a 100-fold decrease of the k_{cat} value.

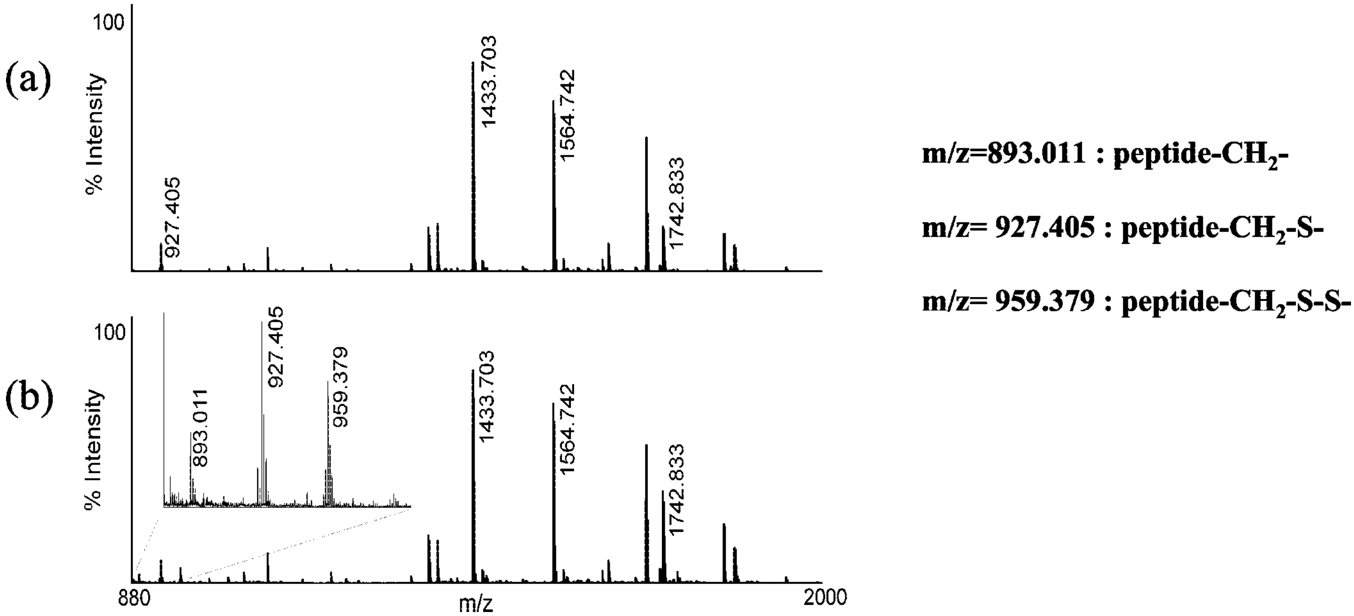

FIG. 4. **MALDI-TOF/TOF MS spectrum of the tryptic peptides of FEZ-1 Y228A (*a*) and FEZ-1 Y228A incubated with cefuroxime (*b*).** The peptide containing the free cysteine Cys[200] (*m/z* 927.48) was found in the active and inactivated enzymes. The peaks at *m/z* of 959.379 and 893.011 indicate the peptides with an extra sulfur atom or after loss of H_2S, respectively.

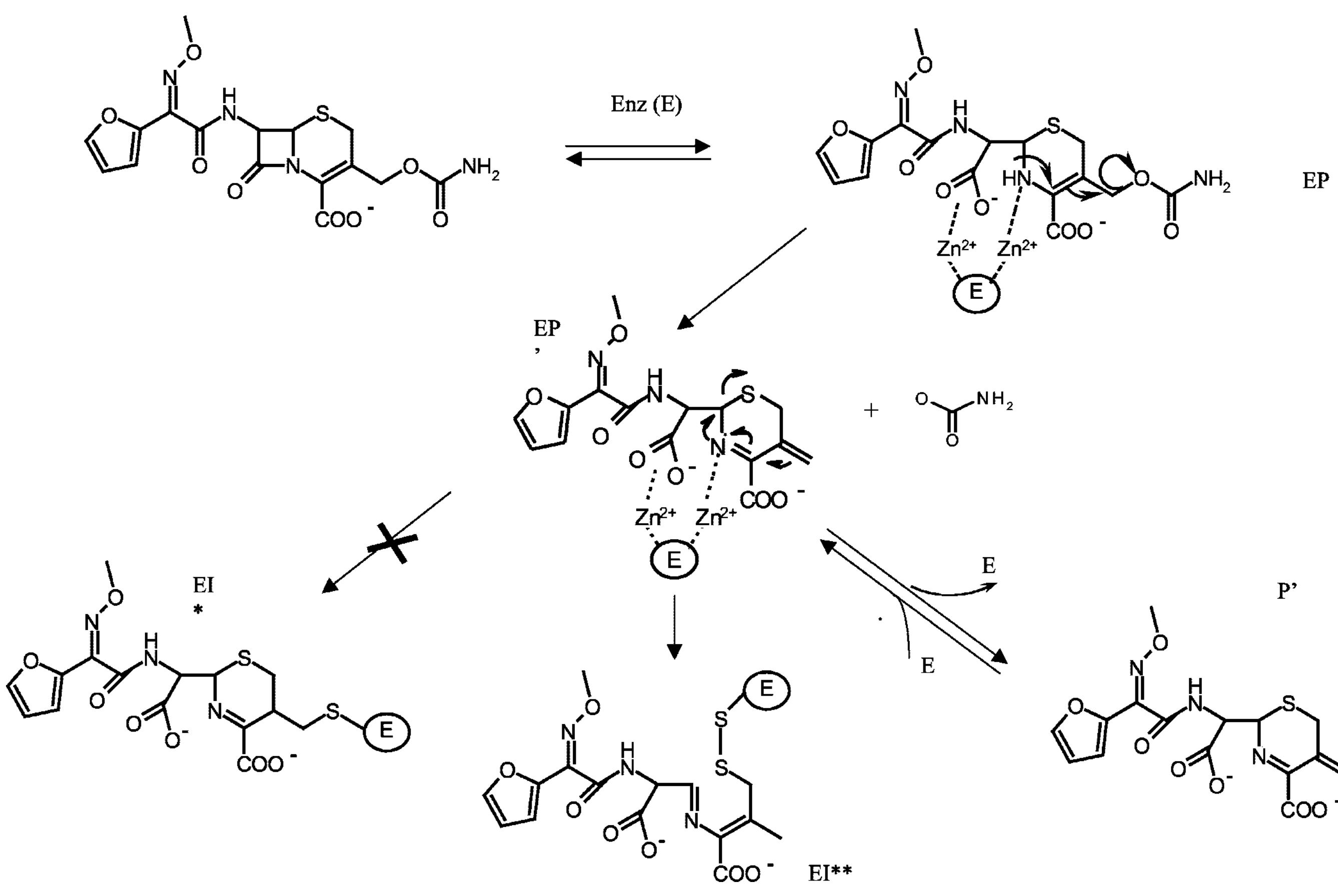

FIG. 5. **Possible mechanism of inactivation of Y228A by cefuroxime.**

Ser[221] is thus not essential for the hydrolysis of cephalosporins and penicillins but plays a more significant role during the hydrolysis of carbapenems. The docking of the penam (for penicillins), the cephem (for cephalosporins), and the carbapenem moieties, respectively, in the active site of the wild type enzyme indicated that the carboxylate group at position C-3 (penicillins and carbapenems) and position C4 (cephalosporins) may interact with the side chain of Ser[221]. In the S221A FEZ-1 mutant, the interaction is not possible and should thus be marked by a clear increase of K_m. This phenomenon was observed in the presence of high zinc ion concentrations in the case of penicillin and cephalosporins. In the case of carbapenems, the absence of the side chain of Ser[221] results in the loss of a strong interaction either with the hydroxyl moiety of the serine side chain or with

TABLE III
X-ray data collection and structure refinement of Y228A FEZ-1 mutant

Parameter	Value
Data collection statistics[a]	
Unit cell dimensions	a = 44.76 Å, b = 77.43 Å, c = 78.50 Å, β = 101.70°
Space group	$P2_1$
Molecules/asymmetric unit	2
Maximum resolution (Å)	2.01
No. of unique reflections	33,715
Overall completeness (%)	97.0
Last shell completeness (%)	88.2[b]
Multiplicity	3.7
R_{sym}[c]	0.063 (0.118)[b]
$I/\sigma(I)$	8.3
Refinement statistics	
No. of reflections	33,305
$R_{working}$[d] (%)	18.6
R_{free}[e] (%)	21.6
Root mean square deviation from ideal	
Bonds (Å)	0.005
Angles (degrees)	1.20

[a] Data collection obtained on an x-ray rotating anode generator Nonius FR-591 coupled to a MarResearch Image Plate at the Laboratory of Macromolecular Crystallography (Grenoble, France).
[b] Last resolution shell: 2.12 to 2.01 Å.
[c] $R_{sym} = \Sigma|I_j - \langle I\rangle|/\Sigma\langle I\rangle$, where I_j is the intensity for reflection j, and $\langle I\rangle$ is the mean intensity.
[d] $R_{working} = \Sigma\|F_o| - |F_c\|/\Sigma|F_c|$, calculated with the working set.
[e] R_{free} was similarly calculated with 9.5% of the data excluded from the calculation of $R_{working}$.

the second water molecule in the active site, which would be necessary in order to have an efficient hydrolysis of the β-lactam.

Kinetic Properties of the Asn[225] Mutant—It has been proposed that the catalytic mechanism of class B β-lactamases involves the hydroxide bridging the two zinc ions, which can serve as the attacking nucleophile on the carbonyl carbon of the β-lactam ring (4). Asn[225] and Zn-1 are likely to form an oxyanion hole that stabilizes the putative tetrahedral intermediate and to contribute to the FEZ-1 catalytic properties. The behavior of N225A was not strongly modified *versus* penicillins (Table II). The catalytic efficiency of the mutant against third generation cephalosporins was even increased compared with the wild type enzyme. The major impact of the mutation was observed on the catalytic properties against carbapenems. With meropenem, the decrease of the k_{cat}/K_m was mainly due to the increase of K_m. For imipenem and biapenem, the k_{cat}/K_m values of N225A were reduced 20-fold. Although the details are somewhat different, at least in the case of meropenem, the properties of both the S221A and N225A mutants underline the fact that the hydrolysis of carbapenems requires the WT active site, whereas that of penicillins and cephalosporins can be catalyzed with conserved efficiency after the elimination of the serine and asparagine side chains at positions 221 and 225, respectively.

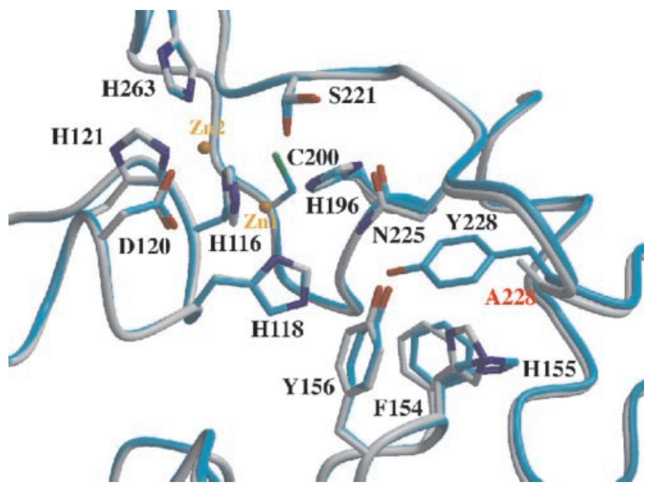

FIG. 6. **Native and Y228A mutant active sites.** Superposition of the crystallographic structures of wild-type FEZ-1 (cyan coil) and the Y228A mutant (*white coil*, Ala[228] marked in *red*). The active site residues and the mutated residues described in this work are labeled. Ser[221] in native FEZ-1 is shown in its double conformation. This figure was generated using BOBSCRIPT (35).

Kinetic Properties of the Y228A Mutant—Tyr[228] does not play a major role in the hydrolysis of penicillins and carbapenems (Table II). The main impact of the mutation was the large increases of the K_m values, which underline a less efficient interaction between the enzyme and its substrate. The steady state kinetic parameters for cefuroxime, cefotaxime, nitrocefin, and cephalothin were estimated by measuring the initial rates of hydrolysis. K_m values for the WT and Y228A were similar and little affected by the presence of zinc ions. By contrast, we noted a large increase of the k_{cat} parameters. As for the WT, the hydrolysis of cefuroxime was not modified in the presence of a large excess of zinc ions, whereas the catalytic constants for cefotaxime and nitrocefin increased by factors of 5 and 16, respectively. Nevertheless, a time-dependent inactivation of the Y228A mutant was observed. In the presence of increasing concentrations of cefuroxime, the rate of enzyme inactivation was dependent on the initial substrate concentration. For a concentration higher than 500 μM, the limit value of the pseudo-first-order rate constant of inactivation was 1.6×10^{-2} s^{-1}. In order to determine whether the inactivation was due to the substrate or the cephalosporin hydrolysis products, the Y228A mutant was incubated in the presence of the hydrolysis product of cefuroxime. It behaved as competitive inhibition (K_i = 140 μM). In addition, prolonged incubation induced the inactivation of the enzyme, and an apparent k_i value of 2.7×10^{-3} s^{-1} was obtained, which was not dependent on the tested hydrolysis product concentrations. These data suggested that the inactivation event is more efficient when the hydrolysis product is generated in the active site of Y228A. The influence of the size of the C7 lateral chain on the formation of inactive enzyme was studied. 7-ACA was similarly hydrolyzed by Y228A and the wild type enzyme (Table II). In addition, no inactivation of the mutant was observed. The difference between cefuroxime and 7-ACA is the presence of a bulky C7 lateral chain (Scheme 1). These data suggest that this lateral chain is essential to the inactivation of the Y228A mutant.

To determine whether the interaction between the hydrolysis product of cephalosporins and the Y228A mutant can lead to a covalent intermediate, ESI-MS was used to monitor the mass increment of the enzyme. The mass spectrum of Y228A is shown in Fig. 2*a*. Two masses were obtained. The mass of 29,358 Da corresponds to the theoretical mass of the Y228A, and the mass of 29,227 Da corresponds to the loss of the N-terminal methionine. After reaction with cefuroxime, mass shifts to 29,739 and to 29,608 Da are observed (Fig. 2*b*). For the WT enzyme, only a small fraction undergoes the mass shift (Fig. 2*c*). This mass increase of 381 Da corresponds well with the mass of hydrolyzed cefuroxime after departure of the 3′ leaving group -NH_2COOH. Such as inactivation mechanism is in good agreement with the reported inactivation of *Aeromonas hydrophila* metallo-β-lactamase CphA by cefoxitin (33). In the latter case, a disulfide bridge is possibly formed between the only cysteine of CphA and the dihydrothiazine sulfur atom of cefoxitin or between the cysteine and the exomethylene group of the hydrolyzed cefoxitin.

ESI-MS of the trypsin-digested enzyme and of the enzyme-cefuroxime complex reveals a doubly charged peptide (*m/z* 654.7) present only in the complex (Fig. 3). The presence of this 1307.4-Da peptide confirms that the Gly^{199}–Lys^{206} peptide (*m/z* 927.5), containing the free cysteine Cys^{200}, binds a cefuroxime fragment of 381 Da. The residue to which the covalent bond is formed could be identified by MALDI-TOF/TOF MS. The Gly^{199}-Lys^{206} peptide (*m/z* 927.5) is observed in both the native enzyme and the complex-derived peptide map (Fig. 4). Two additional peaks at *m/z* 959.5 and *m/z* 893.1, however, are present for the complex (Fig. 4*b*). This 32-Da mass increase and 34-Da mass decrease correspond to the addition of a sulfur atom and the loss of H_2S, respectively. It thus appears that the cefuroxime is linked to the peptide by a disulfide bond. Due to the high laser intensity of the MALDI source, the 1307.4-Da peptide (Gly^{199}–Lys^{206} plus 381-Da cefuroxime fragment) can break in three different positions around the disulfide bond. The 927.5-Da peptide is obtained by the cleavage of the disulfide bond itself (*X*-CH_2-S-). The 893.1-Da peptide is due to the Gly^{199}–Lys^{206} peptide without the cysteine sulfur atom (*X*-CH_2-). Finally, the 959.5-Da peptide corresponds to the peptide containing the disulfide group but not the cefuroxime moiety (*X*-CH_2-S-S-). A similar cleavage of disulfide bridges in MALDI-MS has recently been reported (34). After derivatization of Cys^{200} with iodoacetamide, cefuroxime was no longer able to form a complex with Y228A, showing that the cefuroxime fragment resulting from the departure is indeed bound to this residue (result not shown).

Based on these data, the kinetic scheme of inactivation can be described by a branched pathway (Fig. 5). The hydrolysis of the β-lactam ring proceeds via the formation of noncovalent complexes. The *E*P complex obtained by the interaction between the enzyme and the hydrolysis product of cephalosporins can be transformed in an *E*P′ complex, resulting from the departure of a C-3′ leaving group and the appearance of an exomethylene moiety. *E*P′ can evolve into three different species. The first corresponds to the separation of the free enzyme and the P′ product. The second species is a covalent intermediate obtained by the addition of the free thiol group of Cys^{200} onto the exomethylene group. This reaction gives a stable thioether and was observed with the *A. hydrophila* enzyme but does not seem to occur here. Finally, the third possible dead end intermediate can be obtained by the rupture of the C-6–S-1 bond of the six-membered ring. The reaction yields a free sulfur group that will react with the Cys^{200} side chain to form a stable disulfide bond. Although the opening of the thiazolidine ring seems unlikely, we cannot exclude this possibility based on the analysis of the MS results described above.

Active Site of FEZ-1: Native Form and Y228A Mutant—X-ray data collection and structure refinement of Y228A FEZ-1 mutant are shown in Table III. Except in the vicinity of the mutated Tyr^{228} residue, there are no significant differences between the three-dimensional structures of the wild-type and the mutant enzyme. The active sites of both the wild-type and Y228A mutant enzyme are depicted in Fig. 6. The root mean square deviation between the two main chain atoms (residues 36–311) is 0.18 Å. The main difference between the two structures is at His^{155}, which rotates 94° around the C-γ–C-β bond. This movement affects the neighboring residues Phe^{154} and Tyr^{156}.

We propose that the replacement of the tyrosine side chain by a methyl group, which increases the space in the vicinity of the active site, changes the position of the antibiotic in the catalytic pocket. After hydrolysis of cephalosporins, this space allows a direct interaction between Cys^{200} and the cephem ring, yielding the formation of a covalent and inactive complex. Unfortunately, up to now, we were not able to solve the structure of the Y228A-cefuroxime complex.

CONCLUSIONS

The His^{121} is essential for the production of a dizinc form of FEZ-1 at low zinc concentration. The monozinc enzyme is active and stable. The addition of zinc ion allowed the production of a dizinc enzyme as active as the wild type FEZ-1. All of our data indicate that the main function of His^{121} is to interact with zinc ions. Our studies confirmed that Tyr^{156} does not play an important role in the subclass B3 β-lactamases. Substitutions of Ser^{221} and Asn^{225} modify the activity spectrum of the enzyme. In both cases, the catalytic efficiency of the two mutants against carbapenems decreases. These two residues are involved in the correct positioning of the carbapenem in the catalytic pocket. Finally, we could demonstrate that Tyr^{228} is important in the processing of bulky cephalosporins. The Y228A mutant is inactivated by the hydrolysis product of cephalosporin. Our studies describe the mechanism of inactivation of a subclass B3 enzyme by a β-lactam antibiotic.

Acknowledgment—The atomic absorption measurements were performed by the Laboratoire de la Santé et de l'Environnement, Institut Malvoz de la Province de Liège (Liège, Belgium).

REFERENCES

1. Ambler, R. P. (1980) *Philos. Trans. R. Soc. B Biol. Sci.* **289,** 321–331
2. Bush, K., Jacoby, G., and Medeiros, A. A. (1995) *Antimicrob. Agents Chemother.* **39,** 1211–1233
3. Galleni, M., Lamotte-Brasseur, J., Rossolini, G. M., Spencer, J., Dideberg, O., and Frère, J. M. (2001) *Antimicrob. Agents Chemother.* **45,** 660–663
4. Wang, Z., Fast, W., Valentine, A. M., and Benkovic, S. J. (1999) *Curr. Opin. Struct. Biol.* **3,** 614–622
5. Mercuri P. S., Ishii, Y., Ma, L., Rossolini, G. M., Luzzaro, F., Amicosante, G., Franceschini, N., Frère, J-M., and Galleni, M. (2002) *Microb. Drug Resist.* **8,** 193–200
6. Towns, M. L., Fisher, D., and Moore, J. (1994) *Clin. Infect. Dis.* **8,** 265–266
7. Rossolini, G. M., Condemi, M. A., Pantanella, F., Docquier, J. D., Amicosante, G., and Thaller, M. C. (2001) *Antimicrob. Agents Chemother.* **45,** 837–844
8. Simm A. M., Higgins C. S., Pullan S. T., Avison M. B., Niumsup P., Erdozain O., Bennett P. M., and Walsh T. R. (2001) *FEBS Lett.* **509,** 350–354
9. Docquier, J. D., Pantanella, F., Giuliani, F., Thaller, M. C., Amicosante, G., Galleni, M., Frère, J. M., Bush, K., and Rossolini, G. M. (2002) *Antimicrob. Agents Chemother.* **4,** 1823–1830
10. Carfi, A., Pares, S., Duée, E., Galleni, M., Duez, C., Frère, J. M., and Dideberg, O. (1995) *EMBO J.* **14,** 4914–4921
11. Fabiane, S. M., Sohi, M. K., Wan, T., Payne, D. J., Bateson, J. H., Mitchell, T., and Sutton, B. J. (1998) *Biochemistry* **37,** 12404–12411
12. Concha, N. O., Rasmussen, B. A., Bush, K., and Herzberg, O. (1996) *Structure* **4,** 823–836
13. Garcia-Saez, I., Hopkins, J., Papamicael, C., Franceschini, N., Amicosante, G., Rossolini, G. M., Galleni, M., Frère, J. M., and Dideberg, O. (2003) *J. Biol. Chem.* (2003) **278,** 23868–23873
14. Concha, N. O., Janson, C. A., Rowling, P., Pearson, S., Cheever, C. A., Clarke, B. P., Lewis, C., Galleni, M., Frère, J. M., Payne, D. J., Bateson, J. H., and Abdel-Meguid, S. S. (2000) *Biochemistry* **39,** 4288–4298
15. Ullah, J. H., Walsh, T. R., Taylor, I. A., Emery, D. C., Verma, C. S., Gamblin S. J., and Spencer, J. (1998) *J. Mol. Biol.* **284,** 125–136

16. García-Sáez, I., Mercuri, P. S., Papamicael, C., Kahn, R., Frère, J. M., Galleni, M., Rossolini, G. M., and Dideberg, O. (2003) *J. Mol. Biol.* **325,** 651–660
17. Boschi, L., Mercuri, P.S., Riccio, M. L., Amicosante, G., Galleni, M., Frère, J. M., and Rossolini, G. M. (2000) *Antimicrob. Agents Chemother.* **44,** 1538–1543
18. Mercuri, P. S., Bouillenne F., Boschi, L, Lamotte-Brasseur, J., Amicosante, G., Devreese, B., van Beeumen, J., Frère, J. M., Rossolini, G. M., and Galleni, M. (2001) *Antimicrob. Agents Chemother.* **45,** 1254–1262
19. Crowder, M. W., Walsh, T.R., Banovic, L., Pettit, M., and Spencer, J. (1998) *Antimicrob. Agents Chemother.* **42,** 921–926
20. Felici, A., and Amicosante, G. (1995) *Antimicrob. Agents Chemother.* **39,** 192–199
21. Toney, J. H., Fitzgerald, P. M., Grover-Sharma, N., Olson, S. H., May, W. J., Sundelof, J. G., Vanderwall, D. E., Cleary, K. A., Grant, S. K., Wu, J. K., Kozarich, J. W., Pompliano, D. L., and Hammond, G. G. (1998) *Chem. Biol.* **5,** 185–196
22. Scrofani, S. D., Chung, J., Huntley, J. J., Benkovic, S. J., Wright, P. E., and Dyson, H. J. (1999) *Biochemistry* **38**, 14507–14514
23. Bellais, S., Poirel, L., Leotard, S., Naas, T., and Nordmann, P. (2000) *Antimicrob. Agents Chemother.* **44,** 3028–3034
24. Simm, A. M., Higgins, C. S., Carenbauer, A. L., Crowder, M. W., Bateson, J. H., Bennett, P. M., Clarke, A. R., Halford, S. E., and Walsh, T. R. (2002) *J. Biol. Chem.* **277,** 24744–24752
25. Sambrook, J., Fritsch, E. F., and Maniatis, T. (1989) *Molecular Cloning: A Laboratory Manual*, 2nd Ed., Cold Spring Harbor Laboratory, Cold Spring Harbor, NY
26. De Meester, F., Joris, B., Reckinger, G., Bellefroid-Bourguignon, C., Frère, J. M., and Waley, S. G. (1987) *Biochem. Pharmacol.* **36,** 2393–2403
27. Otwinowski, Z., and Minor, W. (1996) *Methods Enzymol.* **276,** 307–326
28. Collaborative Computing Project 4 (1994) *Acta Crystallogr. Sect. D* **50,** 760–763
29. Brünger, A. T., Adams, P. D., Clore, G. M., De Lano, W. L., Gros, P., Grosse-Kunstleve, R. W., Jiang, J. S., Kuszewski, J., Nilges, M., Pannu, N. S., Read, R. J., Rice, L. M., Simonson, T., and Warren, G. L. (1998) *Acta Crystallogr. Sect. D Biol. Crystallogr.* **54,** 905–921
30. de Seny, D., Heinz, U., Wommer, S., Kiefer, M., Meyer-Klaucke, W., Galleni, M., Frère, J. M., Bauer, R., and Adolph, H. W. (2001) *J. Biol. Chem.* **276,** 45065–45078
31. de Seny, D., Prosperi-Meys, C., Bebrone, C., Rossolini, G. M., Page, M. I., Noel, P., Frère, J. M., and Galleni, M. (2002) *Biochem. J.* **363,** 687–696
32. Carenbauer, A. L., Garrity, J. D., Periyannan, G., Yates, R. B., and Crowder, M. W. (2002) *BMC Biochem.* **3,** 4–10
33. Zervosen, A., Hernandez-Valladares, M., Devreese, B., Prosperi-Meys, C., Adolph, A-W., Mercuri, P. S., Vanhove, M., Amicosante, G., Van Beeumen, J., Frère, J-M., and Galleni, M. (2001) *Eur. J. Biochem.* **268,** 3840–3850
34. Schnaible, V., Wefing, S., Resemann, A., Suckau, D., Bücker, A., Wolf-Kümmeth, S., and Hoffmann, D. (2002) *Anal. Chem.* **74,** 4980–4988
35. Esnouf, R. M. (1999) *Acta Crystallogr. Sect. D* **55**, 938–940
36. Hemmingsen, L., Damblon, C., Antony, J., Jensen, M., Adolph, H. W., Wommer, S., Roberts, G. C., and Bauer, R. (2001) *J. Am. Chem. Soc.* **123,** 10329–10335

Enzyme Catalysis and Regulation:
Probing the Specificity of the Subclass B3 FEZ-1 Metallo- β-lactamase by Site-directed Mutagenesis

Paola Sandra Mercuri, Isabel García-Sáez, Kris De Vriendt, Iris Thamm, Bart Devreese, Jozef Van Beeumen, Otto Dideberg, Gian Maria Rossolini, Jean-Marie Frère and Moreno Galleni
J. Biol. Chem. 2004, 279:33630-33638.
doi: 10.1074/jbc.M403671200 originally published online May 24, 2004